

# Implementation of Digital Twin for Investigation of Delayed Building Construction

Muhammad Rizal Mutaqien<sup>1</sup>, Nurpusparatnasaridewi<sup>1</sup>, Yackob Astor<sup>1\*</sup>,  
Moch. Imam Muflih<sup>1</sup>, Dandi Haniif Pratama<sup>1</sup>, Ananda Amatory Zahra<sup>1</sup>,  
Yasuyuki Nabeshima<sup>2</sup>

<sup>1</sup> Politeknik Negeri Bandung, Civil Engineering Department,  
Jl. Gegerkalong Hilir Ds. Ciwaruga, Kabupaten Bandung Barat, INDONESIA

<sup>2</sup> National Institute of Technology (NIT), Kosen-Akashi College, Civil Engineering Department,  
Nishioka-679-3 Uozumicho, Akashi, Hyogo 674-0084, JAPAN

\*Corresponding Author: [yackobastor@polban.ac.id](mailto:yackobastor@polban.ac.id)

DOI: <https://doi.org/10.30880/ijie.2025.17.09.032>

## Article Info

Received: 27 March 2025

Accepted: 11 August 2025

Available online: 31 December 2025

## Keywords

Terrestrial laser scanner, visual  
damage investigation, non-  
destructive test

## Abstract

During 2020-2022, a significant portion of the national budget was redirected to the healthcare sector for the handling of COVID-19 and economic recovery in Indonesia. This policy has resulted in delays in infrastructure development both nationally and locally. One example is the construction of a government office in Bandung. If construction resumes, investigating the level of damage to structural elements becomes crucial. In this research, the investigation of the level of damage was conducted by constructing a Digital Twin in the form of a 3D building model using the Terrestrial Laser Scanner (TLS) BLK360, Cyclone Register 360 software, and Autodesk Recap Pro. The visual investigation results on the 3D model show the presence of 31 elements, with 39% mild damage and 61% moderate damage out of the total detected damage on columns, beams, and slabs. On the structural element, tests were conducted, with the assistance of the Non-Destructive Test (NDT) equipment, and the examination of the nominal moment capacity strength of the structural elements showed that several elements have experienced damage and a reduction in nominal moment capacity after 3 years construction delayed. On the column there was an increase in nominal moment capacity by 47 kNm and shear strength difference of 5.394 kN. On the Beam, there was a decrease in negative nominal moment capacity, where the value of  $M_n$  actual = 187,067 kNm while the  $M_n$  planned = 241,389 kNm. On floor slab there was a decrease in the nominal moment capacity in the x-direction  $M_n$  actual = 22,984 kNm while the  $M_n$  planned = 28,932 kNm. In the y-direction  $M_n$  actual = 24,167 kNm while the  $M_n$  planned = 22,594 kNm. Based on the investigation results, the delayed building construction can be resumed by repairing and strengthening the damaged structural elements using grouting, epoxy injection, and Fiber-Reinforced Plastic (FRP) methods.

## 1. Introduction

Infrastructure development in Indonesia and other countries was stopped in 2020 and 2021 due to the COVID-19 pandemic, resulting in delays in the completion of several construction projects, with some even being postponed

This is an open access article under the CC BY-NC-SA 4.0 license.



until this year. The government's focus on dealing with a new type of corona virus has caused many infrastructure projects to be delayed. Of the total 208 projects running until April 2020, 13% of them were temporarily suspended or suspended in all parts of the project. Meanwhile, around 23% of projects are in a slowdown condition where there is a slowdown in several parts such as labor mobilization and restrictions on the number of workers in the field due to physical distancing [1]. The stopping of a building construction project can lead to damage to the building, including architectural damage or even structural damage. According to Regulation of the Ministry of Public Works No. 24 of 2008 concerning Guidelines for the Maintenance and Care of Buildings, a building is considered to have experienced damage if the building or its components no longer function due to the end of the building's lifespan, human activity, or natural phenomena [2].

The object of this research is the office building of one of the government agencies in Bandung, West Java. It was constructed in early 2019 and experienced a construction delay of 3 years (Fig 1). This building was situated on 2,513 m<sup>2</sup> of land, with 3 floors, a basement, and a rooftop.

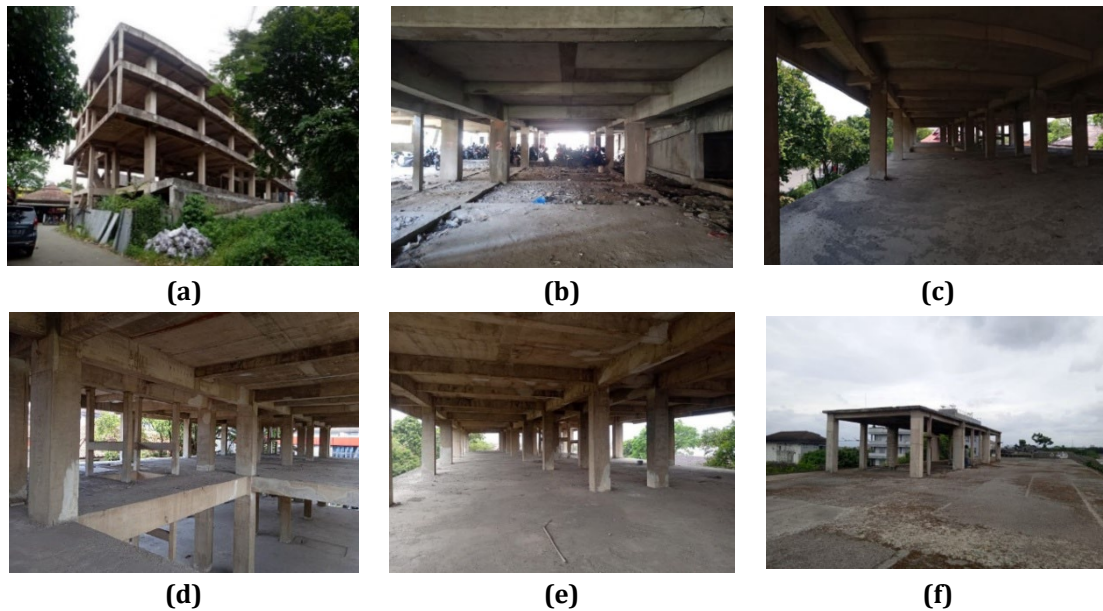


**Fig. 1** Research object (a); Basement (b); 1<sup>st</sup> floor (c); 2<sup>nd</sup> floor (d); 3<sup>rd</sup> floor (e); and rooftop (f)

Based on preliminary visual surveys, the existing condition of the structural elements of the building shows several damages, as indicated in Fig 2. There is water leakage on beams, cracks in beam and column areas, concrete corrosion on columns, deflection in beam areas, and deteriorated concrete revealing reinforcement bars. The condition of the existing building construction indicates structural damage to beam, column, and slab elements. Therefore, before construction work resumes this year, a comprehensive inspection of the existing building is necessary to determine which building components have experienced damage [3].

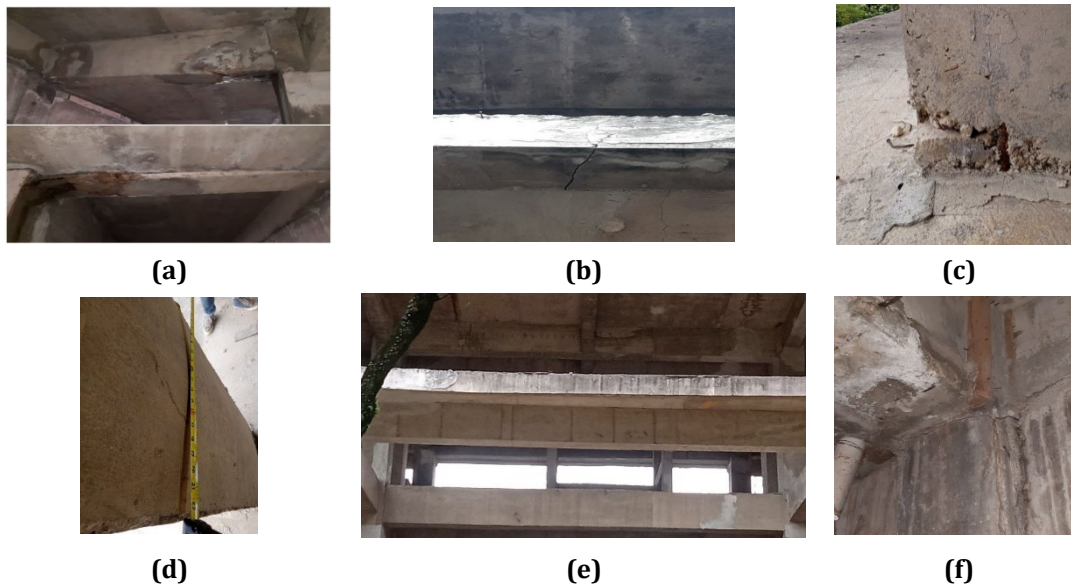


**Fig. 2** *The condition of the building construction after the delay: Water seepage on beam (a); Column crack (b); Hole in the corner beam (c); Column concrete fattening (d); Deflection on column (e); Beam crack (f)*

In general, building inspections are conventionally conducted through surveys, visual observations, and simple measurements recorded manually using forms. Subsequently, calculations are performed to generate values for the level of damage to the building. The efficiency of conventional building inspection work is heavily influenced by the number of personnel, equipment, floors, and the condition of the building [4]. The higher the number of floors, the greater the number of personnel required for building damage inspection. The difficulty often arises when measuring the height of building columns that are inaccessible due to the building's condition or limitations in the capacity of conventional equipment used [5].

The Terrestrial Laser Scanner (TLS) technology serves as a solution to overcome limitations in conventional building damage inspections. In a short amount of time, TLS can scan objects over a wide range, resulting in thousands of points (point clouds) that depict the object realistically (digital twin) [6]. In Indonesia, initially, TLS usage was predominantly for creating Digital Twins of historical buildings such as palaces and temples to observe damages in detail and plan appropriate repair efforts, including maintenance [7]. With the implementation of Building Information Modelling (BIM) concepts in the field of building construction, TLS has become highly valuable for building planning, maintenance, and repair [8]. TLS can be utilized to monitor building safety by identifying structural changes, cracks or other damage; to track construction progress; to help in efficient project management; and to find out overall building condition [8]. It also includes room mapping for interior layout planning, optimizing space utilization, and providing comfort for occupants [9]. Nowadays, the use of TLS is not limited to buildings. Since 2022, TLS has been officially utilized in Special Bridge Inspection activities related to Bridge Geometry Assessment. The provisions for the use of TLS are stated in Ministerial Regulation No. 10 of 2022 concerning the Implementation of Bridge and Road Tunnel Safety [10].

Compared to Indonesia, TLS in several countries has been used more massively and diversely. The use of TLS technology in other countries for buildings has become a common thing. In Europe, TLS is used for mapping and maintaining historical buildings such as ancient structures, palaces, and cathedrals, assisting in documentation and restoration planning [11]. In the United States, TLS is utilized in the construction of tall buildings and infrastructure such as bridges and tunnels to measure dimensions, inspect construction accuracy, and identify potential infrastructure damage issues [12]. In Australia, TLS is utilized for monitoring building structures such as tall buildings and bridges, assisting in detecting changes and damages [13]. In Japan, TLS is utilized in the development of smart cities, including buildings, roads, and other infrastructure [14]. In New Zealand, TLS is utilized for mapping natural environments and buildings, such as forests, beaches, and islands [13]. The use of TLS in other countries has been proven to be beneficial in the management of infrastructure and natural resources [15].

The difference between this research and previous similar research lies in the research object, which is a building that experienced a construction delay of three years and will resume in 2023. This research will develop a digital twin in the form of a 3D model of the building as the primary data for visual investigation of building damages. Furthermore, Non-Destructive Testing (NDT) will be conducted to determine the condition of the structural damage [16]. This research contributes to providing a mechanism for investigating damages to buildings that have experienced construction delays and will resume construction. The mechanisms conducted in

this research can serve as one of the investigation methods in the construction field post the COVID-19 pandemic, both nationally and internationally.

## 2. Materials and Method

The instrument used in this research was the Terrestrial Laser Scanner (TLS) model Leica BLK 360, weighing 0.75 kg including the battery, equipped with wireless connectivity using Wi-Fi or cable via USB-C for faster data transfer, with a storage capacity of 180 GB. The instrument is equipped with LiDAR sensors and has four 13-megapixel cameras capable of capturing 360-degree images. It is also equipped with five High Dynamic Range (HDR) brackets to produce high-contrast images and color accuracy similar to the original. The Leica BLK360 is capable of capturing point clouds at a speed of 680,000 points per second. The accuracy level is at 4 mm at 10 m, with a measurement range extending up to a radius of 45 m. It is equipped with Visual Inertial System (VIS) technology, which automatically combines scanning results from each space throughout the building, thereby integrating each capture to create a complete 3D visualization.

### 2.1 Visual Investigation of Building Damage Through 3D Model

For data acquisition (Fig. 3), it was necessary to determine several standing locations where the scanning process could reach all parts of the object. If scanning at one point was completed, the TLS was then moved to other points until the entire existing building had been scanned. A total of 243 scanning points were conducted for the research object to obtain a complete 3D model.

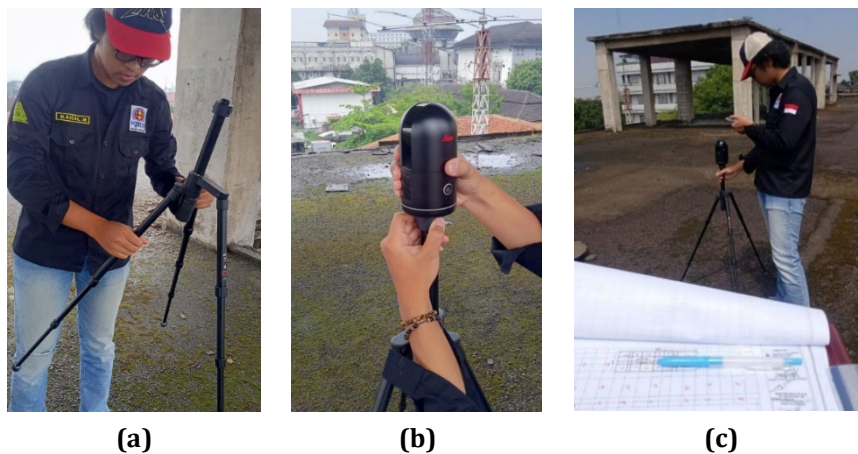


**Fig. 3** The determination of standing locations for the equipment (a); TLS setting (b); The data acquisition process using TLS (c)

The result of data acquisition using TLS is a collection of point cloud data from each station used during the scanning of the object area [17]. The red points in Fig. 4 represent the point cloud data generated from the equipment's standing locations during the object scanning process. It can be observed that the positions of these points are still imprecise and not yet integrated. Therefore, the next step involves the integration of point clouds through a registration process using Cyclone Register 360 software to ensure that the point clouds are in the same coordinate system [18](Fig. 4).

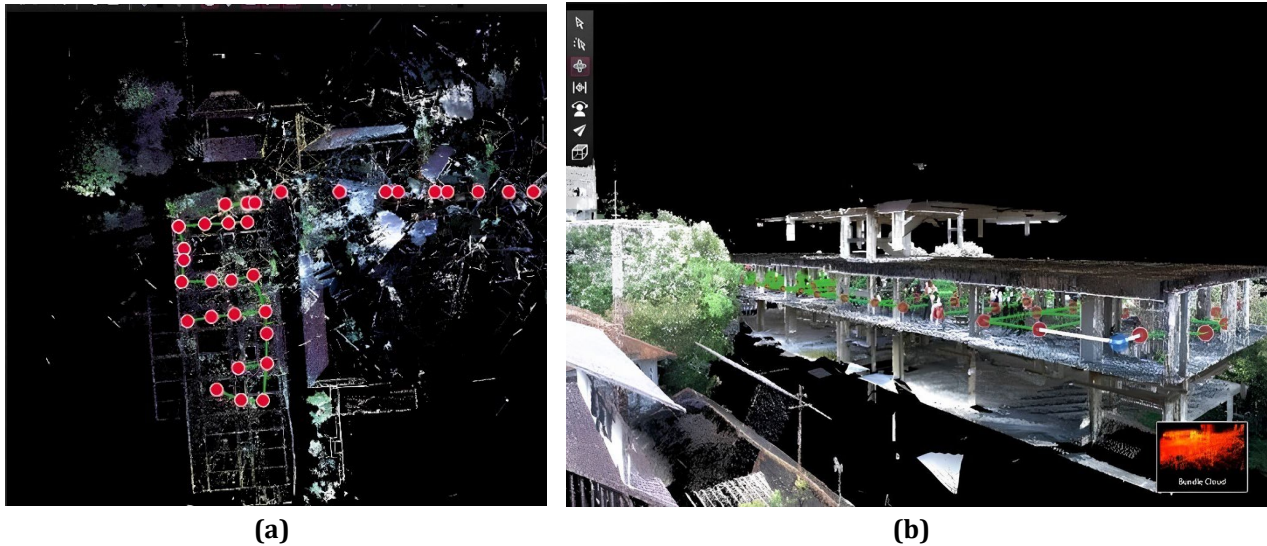
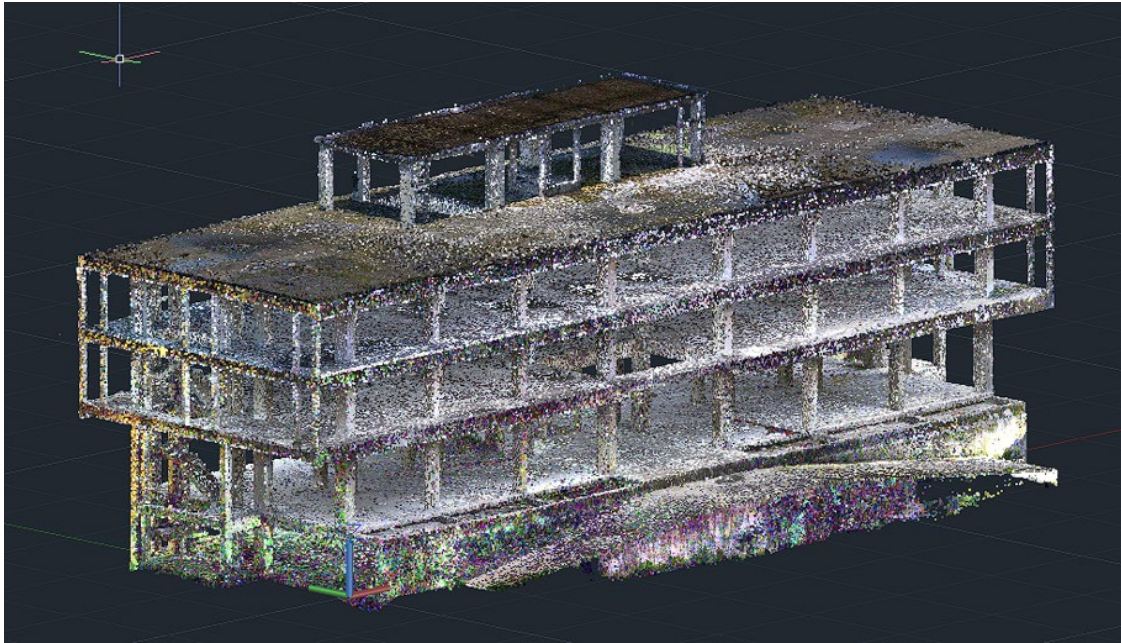


**Fig. 4** Point cloud registration (a); 3D model after registration process (b)

In Fig. 4, the point clouds are seen to be integrated with each other, marked by the presence of green lines connecting each point. This results in the formation of a 3D model of the existing building, which serves as the scanning object [19]. However, in Fig. 4, there is still a significant amount of noise around the main building, such as trees, people, and surrounding structures that were scanned by the TLS device during data acquisition [20]. Therefore, a filtering process is necessary by selecting objects that need to be retained and removing some objects to produce a complete 3D model of the building, thus improving the quality of the 3D model visualization [21]. At this stage, the filtering process of the point cloud data was conducted using Autodesk Recap Pro software. Fig. 5 shows the 3D model before and after filtering. The filtering results clarify the 3D model and retain the main objects for visual investigation of building damages [22].



**(a)**



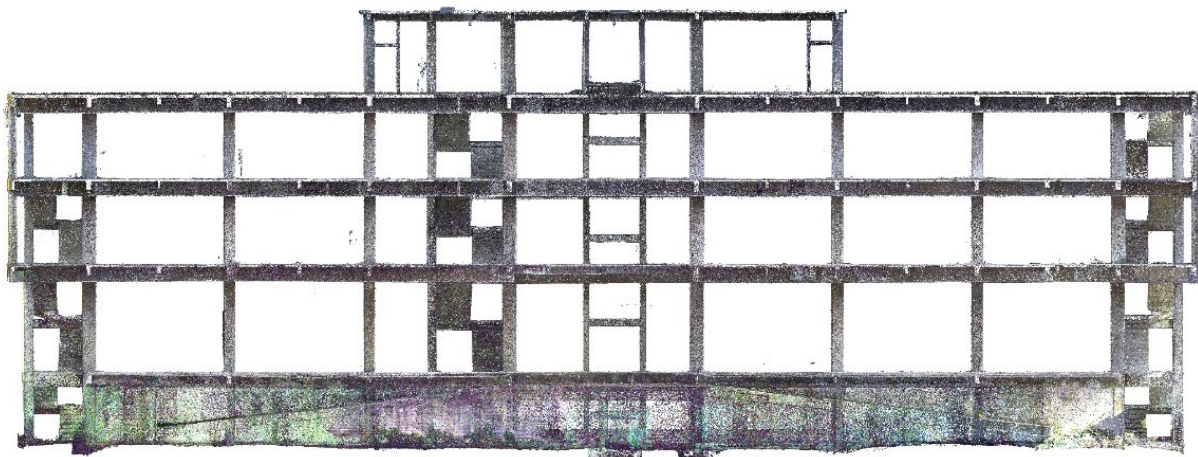
(b)

**Fig. 5** The 3D model before the filtering process (a); and after the filtering process (b)

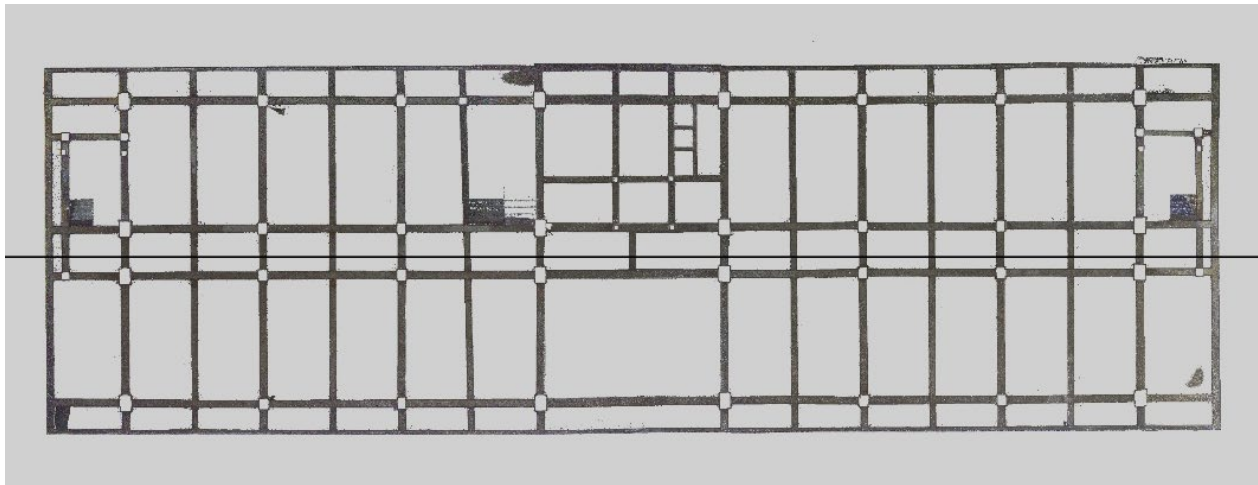
The final stage involves the Meshing process to convert the collection of 3D points into a solid 3D surface model so that it can be used for visual investigation of building damages [23]. The investigation was conducted by identifying and inventorying the types of damage on the model, which were then validated based on the actual field conditions. Subsequently, the results of the visual investigation are evaluated by the Guidelines of the Ministry of Public Works and Spatial Planning of the Republic of Indonesia No. 16 of 2010 Chapter III concerning Types of Damage, as well as Circular Letter Number 12/SE/Dr/2022 Chapter IV sub-chapter 4.3.1 regarding Damage Level Categories [24].

## 2.2 The Creation of As-Built Drawings from 3D Model

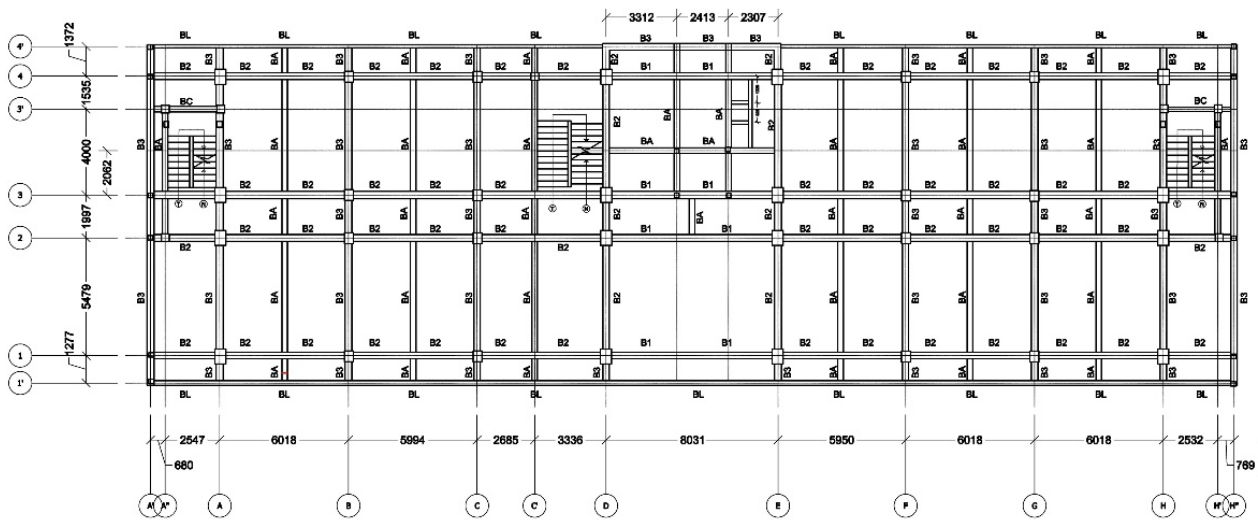
At this stage, the 3D model was transformed into a 2D model presented in the form of as-built drawings of the existing building (Fig. 6). The transformation process was conducted using the Autodesk AutoCAD software [17]. The creation of as-built drawings from a 3D model is one of the advantages of using TLS in the construction field [25]. In this research, 4 (four) as-built drawings were produced for the basement, each floor, and the rooftop.



(a)



(b)



(c)

**Fig. 6** As-built drawing from the model 3D resulting from TLS: 3D model front view(a); 2D model top view (b); As-built drawing (c)

The creation of as-built drawings from the TLS 3D model aims to determine the conformity with the previously made as-built drawings by the contractor [26]. The conformity referred to includes dimensional values, Axis-to-Axis distances, and the number of reinforcements.

### 2.3 Comparing Dimension Values and Axis-to-Axis Distance

In this research, a comparison of conformity was conducted among the as-built drawing from 2019, the as-built drawing resulting from the 3D model in 2023, and the field measurements in 2023. This comparison is carried out to determine the suitability of dimensional values and axis-to-axis distances.

### 2.4 Damage Investigation through Non-Destructive Testing (NDT)

Non-Destructive Test (NDT) is a testing method without damaging the material that aims to determine that exists on an object. In this research, NDT is used to find damage in an object that cannot be investigated visually by TLS because TLS only models all visible objects (not transparent objects). NDT tests were conducted on column, beam, and slab elements following ASTM C876-91: Standard Test Method for Half-Cell Potential of Uncoated Reinforcing Steel in Concrete.

In this research, three NDT tests were conducted [27]:

- Ultrasonic Pulse Velocity (UPV) Test
- Rebar Locator Test
- Rebar Corrosion Tester Test

The Ultrasonic Pulse Velocity (UPV) test aims to determine the concrete density, depth of cracks in concrete structures, and concrete compressive strength. The testing method involves the propagation of waves with a propagation time on the object's surface at a specific distance, ensuring no damage to the object being tested [28]. Fig. 7 shows the equipment used, including the Pundit, Transducer, and Calibration Bar. The UPV test was conducted on beams, columns, and floor slabs.

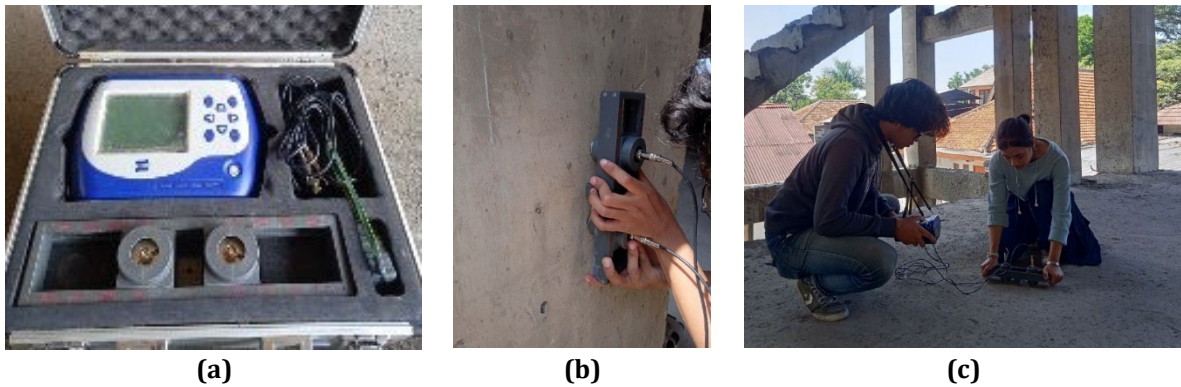


**Fig. 7** The equipment (a); UPV test on column (b); UPV test on floor slabs (c)

The Rebar Locator test using a Profometer was conducted on concrete column, beam, and floor slab structures (Fig. 8), with each dimension representing one sample, to determine the comparison between the actual number of reinforcements in the field and the as-built drawing [29]. The data was processed using ProVista software.

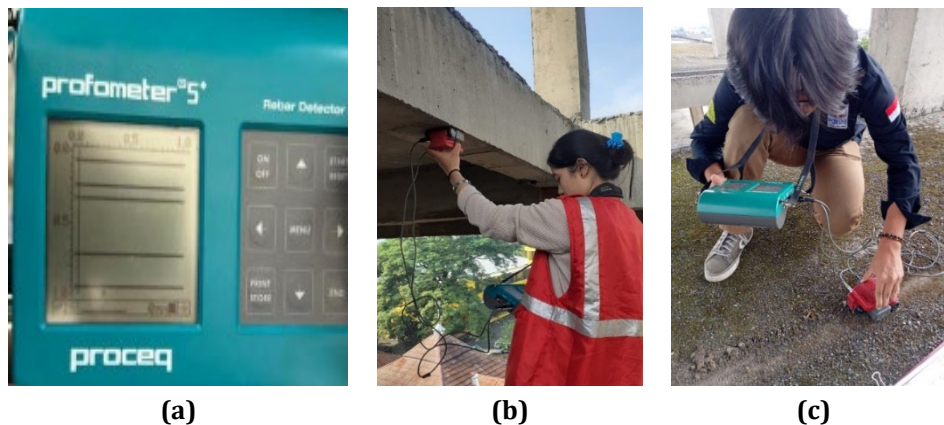


**Fig. 8** Profometer (a); Steel reinforcement data acquisition on column (b); and floor slab (c)

The Rebar Corrosion Tester (Canin) test aims to calculate the corrosion value of steel reinforcement in concrete [30]. The measurement was conducted at marked points being tested with a 5 cm distance horizontally and vertically according to the direction of the reinforcement being tested, with 6-12 testing points (Fig. 9). The measurement was conducted with the foam condition on the tube being moistened by  $\text{CuSO}_4$  liquid, enabling the testing, with the negative valve placed on the  $\text{CuSO}_4$  and the positive valve on the reinforcement protruding from the concrete [31].

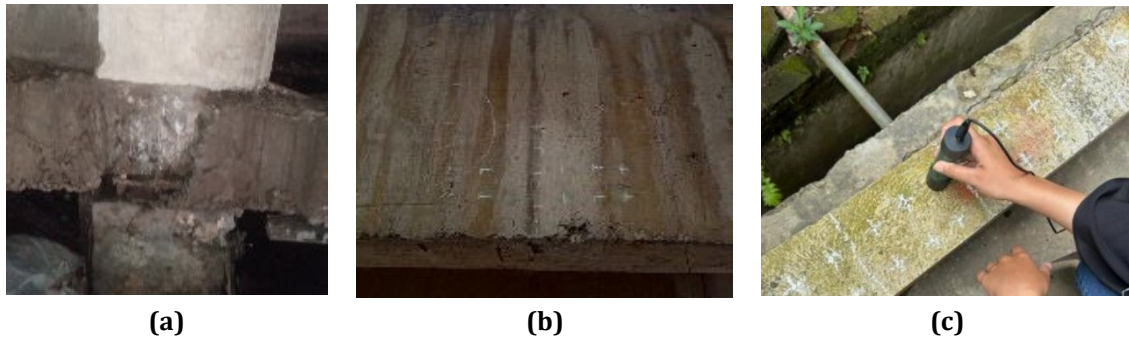


**Fig. 9** Structural in saturated water condition (a); Canin test point marking (b); Rebar corrosion tester on beam (c)

### 3. Result and Discussion

From the visual investigation results, 31 locations of damage on the structural elements were obtained, classified into 2 categories:

- a. Light damage in 12 elements, or 39%.
  - Light damage on column elements: hairline cracks on the upper part of the column and grouting, cracks and corrosions at the column-beam joints.
  - Light damage on beam elements: corrosions, cracks, spalls, beam dimension expansion, and beam corrosion.
- b. Moderate damage in 19 elements, or 61%.
  - Moderate damage on column elements: voids on the upper part of the column, corrosions revealing reinforcement, corrosions on the top part, and water seepage.
  - Moderate damage on beam elements: water seepage at beam-column junctions, leakage at plate-beam connections, cracks, and corrosion revealing reinforcement.
  - Moderate damage on plate elements: cracks, cracks revealing reinforcement.

In this research, the 3D model generated using TLS cannot fully be utilized for the identification of building damage types according to the Guidelines of the Minister of Public Works and Spatial Planning of the Republic of Indonesia No. 16 of 2010 Chapter III concerning Types of Damage [24].



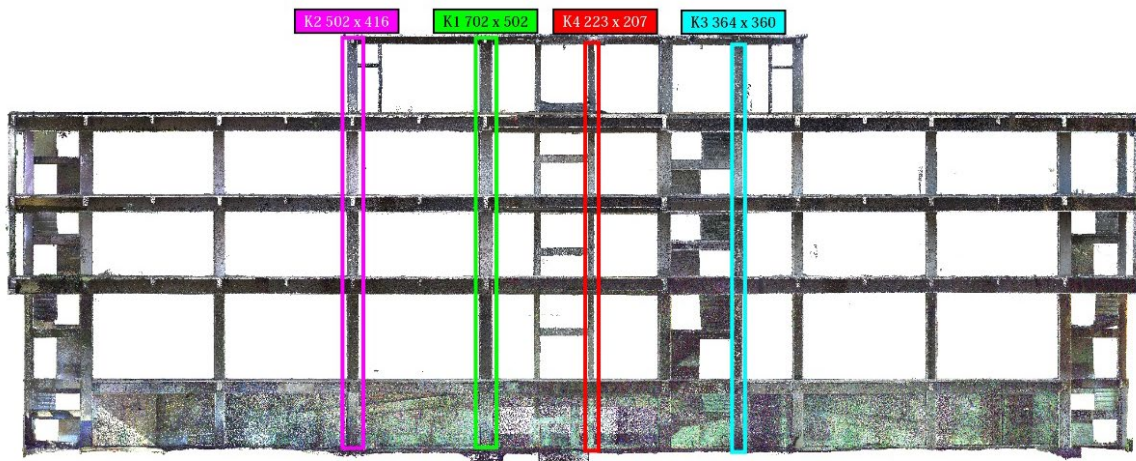
**Fig. 10** Comparison of damage visualization on field object and 3D model

Fig. 10 shows a comparison of damage visualization in the field and the 3D model in two views. In the 3D model (real colour), no damage is visible on the column element. The use of false colour can reveal the presence of damage, but it is difficult to identify the type of damage [32]. This condition is influenced by at least two main factors:

1. The location of damage on the column is too far from the radius of the instrument's standing location, especially for damage located at the outer end of the building. To improve the results, it is necessary to acquire excess data while ensuring that the overlap between the radius of the instrument's standing locations is above 60% [33]. Overlap aims to increase the number of points with a higher density of points.

- The conversion process from point clouds to solid 3D models significantly affects the visual quality of building damage. It requires the use of more powerful software applications or more appropriate methods. The voxelization method based on points automatically transforms point cloud data into solid models using computational modelling [34].

In addition to the visual comparison of building damage above, a dimensional comparison was also conducted on the TLS-derived 3D model against field measurement data and secondary data. The TLS-derived 3D model was converted into the latest as-built drawing for the year 2023 and compared with the as-built drawing from 2019, as well as measurement data using a tape measure for the year 2023, which is assumed to be correct or has minimal errors. The dimensional comparison was conducted on column elements (Table 1 and Fig. 11), beams (Table 2 and Fig. 12), and the distance from axis to axis (Table 3 and Fig. 13).



**Fig. 11** Location of column K1-K4

**Table 1** Results of the dimensional as-built drawing comparison on column elements

Element Type	Column Dimension Description (mm)		
	As-Built Drawing 2019	As-Built Drawing 2023	Manual Measurement
Column K1	700 × 500	702 × 516	709 × 502
Column K2	500 × 400	502 × 416	501 × 410
Column K3	350 × 350	364 × 360	359 × 355
Column K4	200 × 200	223 × 207	215 × 214

Based on the data in Table 1, the dimensions of the columns measured using TLS tend to be larger than the other two comparison objects. Although there are differences in dimension values among the comparison objects, these differences are not significant. The largest difference in dimension values recorded is 23 mm.

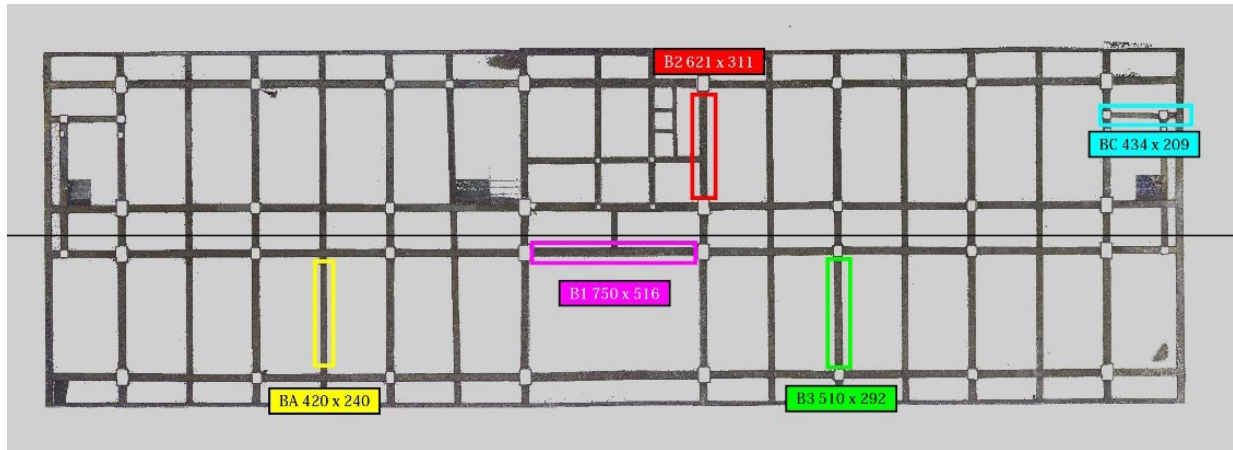


**Fig. 12** Location of beam B1, B2, B3, BA, & BC

**Table 2** Results of the dimensional as-built drawing comparison on beam elements

Element Type	Beam Dimension Description (mm)		
	As-Built Drawing 2019	As-Built Drawing 2023	Manual Measurement
Beam B1	750 × 350	750 × 362	752 × 355
Beam B2	600 × 300	621 × 311	605 × 303
Beam B3	500 × 300	510 × 292	507 × 201
Beam BA	400 × 250	420 × 240	403 × 256
Beam BC	400 × 200	434 × 209	402 × 204

In Table 2, the dimensions of the beams measured using TLS tend to be larger than the other two comparison objects. Although there is variation in dimension values among the comparison objects, these differences are not significant. The largest difference in dimension values recorded is 34 mm.



**Fig. 13** Location of axis to axis

**Table 3** Results of the as-built drawing comparison for axis-to-axis distance

Axis Location	Axis-to-Axis Distance Description (mm)		
	As-Built Drawing 2019	As-Built Drawing 2023	Manual Measurement
A"-A	2.575	2.547	2.572
A-B	6.000	6.018	6.009
B-C	6.000	5.994	6.005
C-C'	2.700	2.685	2.703
C'-D	3.300	3.336	3.304
D-E	8.000	8.031	8.006
E-F	6.000	5.950	5.997
F-G	6.000	6.018	6.000
G-H	6.000	6.018	6.002
H-H'	2.575	2.532	2.568
1'-1	1.250	1.277	1.247
1-2	5.500	5.479	5.493
2-3	2.000	1.997	2.000
3-3'	4.025	4.000	4.018
3'-4	1.475	1.535	1.484
4-4'	1.400	1.372	1.395

Table 3 shows that the as-to-as distance measured using TLS tend to be larger than the other two comparison values. Although there is variation in the distance values among the comparison objects, these differences are not significant [35]. The largest difference in as-to-as distance recorded is 60 mm.

The three tables above (Tables 1-3) show a pattern where the values in the as-built drawing from the TLS 3D Model tend to be larger than the other two comparative values. This is influenced by the point cloud filtering process, which was not optimal, which was carried over during the conversion process from 3D model to 2D (As Build Drawing) [36]. The spatial resolution of the TLS used also significantly affects the resulting 3D Model. This is also true during the Meshing process, which involves converting a collection of 3D points into a solid 3D surface model [37]. However, in general, the comparison of values shown in the three tables above predominantly has insignificant differences, or it can be said that the use of TLS for measuring the distance and dimensions of columns/beams has a larger size [38].

To investigate structural damage, NDT tests were conducted, consisting of three tests, which are the Ultrasonic Pulse Velocity (UPV) test, the Rebar Locator test, and the Rebar Corrosion Tester test [39].

The test results in this research were compared with the data from 2019 to determine the extent of the differences that occurred after the building construction was delayed for 3 years:

- Column (nominal moment comparison): in the capacity calculation of column K2 using SpColumn with dimensions of 500 x 400, there was an increase in nominal moment capacity by 47 kNm, proven by the value of  $M_{nb}$  from NDT  $> M_{nb}$  planned by the contractor, where the value of  $M_{nb}$  from NDT = 299 kNm while the planned  $M_{nb} = 252$  kNm.
- Column (Shear Strength Comparison): based on the calculation data obtained from the as-built drawing,  $\emptyset V_n$  from the planned  $P_{nb}$  result was 499,797 kN, while  $\emptyset V_n$  from the actual  $P_{nb}$  result was 504,798, resulting in a shear strength difference of 5,001 kN. For the actual calculation of the field test results using NDT, the  $\emptyset V_n$  obtained from the planned  $P_{nb}$  result was 491,937 kN and 497,331 from the actual  $P_{nb}$ , resulting in a shear strength difference of 5,394 kN.
- Beam: in the capacity calculation of beam element B3 at the support and field area, there was a decrease in negative nominal moment capacity, proven by the value of  $M_n^-$  actual  $< M_n^-$  planned, where the value of  $M_n^-$  actual = 187,067 kNm while the  $M_n^-$  planned = 241,389 kNm.
- Floor slab: in the capacity calculation of slab element As E-F/1-2 in the x-direction, there was a decrease in the nominal moment capacity, proven by the value of  $M_n$  actual  $< M_n$  planned, where the value of  $M_n$  actual = 22,984 kNm while the  $M_n$  planned = 28,932 kNm. in the capacity calculation of slab element As E-F/1-2 in the y-direction, there was a decrease in the nominal moment capacity, proven by the value of  $M_n$  actual  $< M_n$  planned, where the value of  $M_n$  actual = 24,167 kNm while the  $M_n$  planned = 22,594 kNm.

The results of this study reinforce Lai's research in 2023 that the 3D model produced by TLS can provide good dimensional visualization of an object in the form of a suspension bridge [11]. Although TLS can provide 3D visualization of objects, this is not enough. For a building investigation work really requires tests related to building structures to determine the condition and damage of a material contained in the building which TLS is unable to reach. The use of TLS is done to replace conventional visual investigation activities. In addition, the product produced by TLS in the form of a 3D Model can provide a comprehensive visualization that describes the current existing condition of the building after three years of delayed construction. This is the most important point in this research, in addition to the structural investigation using NDT for the entire building.

In this research, the products of TLS in the form of 3D models and NDT test data are still separate and not integrated. Some researchers have integrated these two outputs into a complete information system. In Lai's research, NDT test results were integrated into the 3D model by displaying visualization in the form of color intensity. Another study integrated the 3D model with bridge damage data including rust [40].

#### 4. Conclusion and Contribution

Based on the discussion above, the investigation of visual and structural damage is crucial for buildings that have experienced a construction delay of three years and will resume construction. The investigation of visual damage using a digital twin in the form of a 3D model generated by TLS is capable of identifying various types of damage, enabling inventory and classification based on the level of damage according to applicable guidelines. Although some damaged objects are difficult to identify, this issue can be addressed through various means, including data acquisition strategies using closer radius, more powerful data processing applications, and the use of TLS with higher technical specifications. The object of this research is limited to a building with 3 floors, 1 basement, and a rooftop. If the object in the field is a building with more than 10 floors with many rooms, then a digital twin is indeed a highly suitable solution for visual investigation.

The novelty of this article is the use of the Building Information Modeling (BIM) 3D for visual damage investigations and structural investigation using NDT for delayed building construction. This research demonstrates that in addition to visual damage investigation, structural damage investigation is also crucial. The results of NDT tests and checking the strength of the nominal moment capacity of structural elements against several elements indicated damages and decreased nominal moment capacity. Repair is necessary using grouting or epoxy injection methods, as well as Fiber-Reinforced Plastic (FRP). This method is relatively easy to implement for mild and moderate levels of damage to repair cracks, spalling, and leaks in concrete. The investigation conducted in this research is comprehensive and essential in the construction field, particularly for the maintenance and repair of infrastructure. Based on the results of the investigation, the delayed building construction can be resumed by repairing and strengthening the damaged structural elements.

The development of this research can be directed towards data acquisition processes using TLS conducted in a time series manner so that the visualization of building damage can be seen over time. Not only showing the visualization of worsening damage but is also accompanied by the increasing dimensions of damage. The time series data acquisition using TLS is easy, fast, and does not require many resources. Digital Twin is not only used for buildings that experience construction delays or buildings that have completed construction and are operational but can also be done during construction so that the estimated time can be determined whether the work is showing progress as expected and can be completed on time. Further research lies in the technology and type of TLS used. This research employs a static TLS method, considering the instrument's radius, thus requiring placement at multiple points to reach all sides of the object. This condition is unnecessary when using the dynamic TLS method, where the instrument can simply be held, allowing data recording while walking through all corners of the object. Another challenge from this research is how to integrate 3D Models that display visualizations of building conditions with information on structural investigation results using NDT for buildings of more than one floor. Increasing the BIM level from the 3D level to the next level, namely 4D and 5D, has become a challenge for research into modelling facilities and infrastructures.

#### Acknowledgement

This research is funded by Research and Community Service Center of Politeknik Negeri Bandung.

#### Conflict of Interest

Authors declare that there is no conflict of interest regarding the publication of the paper.

## Author Contribution

The authors confirm contribution to the paper as follows: **study conception and design:** Muhammad Rizal Mutaqien, Nurpusparatnasaridewi, Yackob Astor and Yasuyuki Nabeshima; **data collection:** Muhammad Rizal Mutaqien, Nurpusparatnasaridewi, Moch. Imam Muflih; **analysis and interpretation of results:** Muhammad Rizal Mutaqien, Nurpusparatnasaridewi, Dandi Haniif Pratama, Ananda Amatory Zahra; **draft manuscript preparation:** Dandi Haniif Pratama, Ananda Amatory Zahra. All authors reviewed the results and approved the final version of the manuscript.

## References

- [1] Sidik, S. (2020) *Dampak Covid-19, proyek WIKA mangkrak & laba bisa drop 50%* [Internet]. CNBC Indonesia, <https://www.cnbcindonesia.com/market/20200528141824-17-161514/dampak-covid-19-proyek-wika-mangkrak-laba-bisa-drop-50>
- [2] Peraturan Menteri Pekerjaan Umum. (2008) *Peraturan Menteri Pekerjaan Umum No 24/PRT/M/2008 tentang Pedoman Pemeliharaan dan Perawatan Bangunan Gedung*.
- [3] Maharfi, E. D., Arief, T., & Purbasari, D. (2019) Studi pemanfaatan teknologi terrestrial laser scanner untuk menghitung volume pengupasan overburden di Pit 2 Elektrifikasi Banko Barat PT. Bukit Asam, Tbk. Tanjung Enim, Sumatera Selatan. *Prosiding Temu Profesi Tahunan PERHAPI*, 1(1), 47–60.
- [4] Tomczyk, M., & van der Valk, H. (2022) Digital twin paradigm shift: The journey of the digital twin definition. In *International Conference on Enterprise Information Systems (ICEIS) – Proceedings*, 2, 90–97.
- [5] Sukmono, A., Putra, F. A., Bashit, N., & Nugraha, A. L. (2021) Utilization of terrestrial laser scanning data in building information modelling (BIM) for fire disaster evacuation simulation, *Civil Engineering and Architecture*, 9(7), 2129–2139, <https://doi.org/10.13189/cea.2021.090702>
- [6] Gumilar, I., Stiawan, A., Bramanto, B., Mulyadi, B., & Abidin, H. Z. (2019) Assessment on topographic mapping using total station and terrestrial laser scanner technology (Case study: Kiara Payung area, Sumedang), *IOP Conference Series: Earth and Environmental Science*, 389, 012006, <https://doi.org/10.1088/1755-1315/389/1/012006>
- [7] Suwardhi, D., Mukhlisin, M., Darmawan, D., Trisyanti, S. W., Brahmantara, B., & Suhartono, Y. (2016) Survey dan pemodelan 3D (tiga dimensi) untuk dokumentasi digital Candi Borobudur, *Jurnal Konservasi Cagar Budaya*, 10(2), 10–22, <https://doi.org/10.33374/jurnalkonservasicagarbudaya.v10i2.150>
- [8] Rianty, N. D. (2021) Optimalisasi teknologi terrestrial laser scanner (TLS) dalam pembuatan building information model (BIM) (Studi kasus: Gedung Dekanat Baru Fakultas Teknik, Universitas Diponegoro), *Jurnal Geodesi Undip*, <https://ejournal3.undip.ac.id/index.php/geodesi/article/view/31320>
- [9] Nandaru, A., Sudarsono, B., & Yuwono, D. (2014) Studi registrasi point cloud pada pemrosesan data terrestrial laser scanner (TLS) (Studi kasus: Jembatan Gading Batavia, Kelapa Gading, Jakarta Utara), *Jurnal Geodesi Undip*, 3(4), 201–211, <https://doi.org/10.14710/jgundip.2014.6816>
- [10] Kementerian Pekerjaan Umum dan Perumahan Rakyat. (2022) *Peraturan Menteri Pekerjaan Umum dan Perumahan Rakyat Republik Indonesia Nomor 10 Tahun 2022 tentang Penyelenggaraan Keamanan Jembatan dan Terowongan Jalan*.
- [11] Liu, J., Azhar, S., Willkens, D., & Li, B. (2023) Static terrestrial laser scanning (TLS) for heritage building information modeling (HBIM): A systematic review, *Virtual Worlds*, 2(2), 90–114, <https://doi.org/10.3390/virtualworlds2020006>
- [12] Sroczyńska, J. (2022) Preventive maintenance of historical buildings in European countries – Analysis of selected examples, *Architectus*, 2(70), 51-57, <https://doi.org/10.37190/arc220205>
- [13] Beach, M., Sadikin, H., Andreas, H., & Suherman, A. P. (2017) Land parcel 3D mapping using terrestrial laser scanning (TLS), case study: Mutiara Beach, Jakarta, Indonesia (8894)
- [14] Sanhudo, L., Ramos, N. M. M., Martins, J. P., Almeida, R. M. S. F., Barreira, E., Simões, M. L. & Cardoso, C. (2020) A framework for in-situ geometric data acquisition using laser scanning for BIM modelling, *Journal of Building Engineering*, 28, 101073, <https://doi.org/10.1016/j.jobe.2019.101073>
- [15] Rashidi, M., Mohammadi, M., Kivi, S. S., Abdolvand, M. M., Truong-Hong, L., & Samali, B. (2020) A decade of modern bridge monitoring using terrestrial laser scanning: Review and future directions, *Remote Sensing*, 12(22), 3796, <https://doi.org/10.3390/rs12223796>
- [16] Xiong, R., & Tang, P. (2021) Pose guided anchoring for detecting proper use of personal protective equipment. *Automation in Construction*, 130, 103828, <https://doi.org/10.1016/j.autcon.2021.103828>

- [17] Shim, S., Kim, J., Lee, S. W., & Cho, G. C. (2021) Road surface damage detection based on hierarchical architecture using lightweight auto-encoder network, *Automation in Construction*, 130, 103833, <https://doi.org/10.1016/j.autcon.2021.103833>
- [18] Abbas, M. A., Luh, L. C., Setan, H., Majid, Z., Chong, A. K., Aspuri, A., et al. (2014). Terrestrial laser scanners pre-processing: Registration and georeferencing, *Jurnal Teknologi*, 71(4), 2180-3722, <https://doi.org/10.11113/jt.v71.3833>
- [19] Zakaria, M. H., Idris, K. M., Majid, Z., Ariff, M. F. M., Darwin, N., Abbas, M. A., Zainuddin, K., Shukor, R. A. & Aziz, M. A. (2019). Practical terrestrial laser scanning field procedure and point cloud processing for BIM applications – TNB control and relay room 132/22KV, *ISPRS Archives*, 42(4/W16), 705–710.
- [20] Uggl, G., & Horemuz, M. (2021). Towards synthesized training data for semantic segmentation of mobile laser scanning point clouds: Generating level crossings from real and synthetic point cloud samples, *Automation in Construction*, 130, 103839, <https://doi.org/10.1016/j.autcon.2021.103839>
- [21] Ho, M. C., Lin, J. D., & Huang, C. F. (2020) Automatic image recognition of pavement distress for improving pavement inspection, *International Journal of GEOMATE*, 19(71), 242–249, <https://doi.org/10.21660/2020.71.96640>
- [22] Almukhtar, A., Saeed, Z. O., Abanda, H., & Tah, J. H. M. (2021) Reality capture of buildings using 3D laser scanners, *CivilEng*, 2(1), 214–235, <https://doi.org/10.3390/civileng2010012>
- [23] Arayici, Y. (2007) An approach for real world data modelling with the 3D terrestrial laser scanner for built environment, *Automation in Construction*, 16(6), 816–829, <https://doi.org/10.1016/j.autcon.2007.02.008>
- [24] Kementerian Pekerjaan Umum (2010) *Peraturan Menteri Pekerjaan Umum No. 16 Tahun 2010 tentang Pedoman Teknis Pemeriksaan Berkala Bangunan Gedung*, <https://peraturan.bpk.go.id/Details/160054/permen-pupr-no-16prtm2010-tahun-2010>
- [25] Feng, H., Chen, Q., & de Soto, B. G. (2021) Application of digital twin technologies in construction: An overview of opportunities and challenges, *Proceedings of the International Symposium on Automation and Robotics in Construction*, 979–986, <https://doi.org/10.22260/ISARC2021/0132>
- [26] Thomas, R. V., Nair, D. G., & Enserink, B. (2023) Conceptual framework for sustainable construction, *Architecture, Structures and Construction*, 3(1), 129–141, <https://doi.org/10.1007/s44150-023-00087-8>
- [27] Isro, E. S., Shar, S., & College, J. (2020) Half cell potential studies for durability studies of concrete structures in coastal environment, *Special Issue of e-Journal of Nondestructive Testing (eJNDT)*, 26(4), 1435-4934
- [28] Pangestu, S. F., & Pratama, M. M. A. (2021) Evaluasi kinerja struktur gedung bertingkat menggunakan pendekatan desain berbasis kinerja. *Cantilever: Jurnal Penelitian dan Kajian Bidang Teknik Sipil*, 10(2), 91–100, <https://doi.org/10.35139/cantilever.v10i2.110>
- [29] Russhakim, N. A. S., Ariff, M. F. M., Darwin, N., Majid, Z., Idris, K. M., Abbas, M. A., Zainuddin, N. K. & Yusoff, A. R. (2018) The suitability of terrestrial laser scanning for strata building, *ISPRS Archives*, 42(4/W9), 67–76, <https://doi.org/10.5194/isprs-archives-XLII-4-W9-67-2018>
- [30] Rogeau, N., Latteur, P., & Weinand, Y. (2021) An integrated design tool for timber plate structures to generate joints geometry, fabrication toolpath, and robot trajectories, *Automation in Construction*, 130, 103875, <https://doi.org/10.1016/j.autcon.2021.103875>
- [31] Jones, D., Snider, C., Nassehi, A., Yon, J., & Hicks, B. (2020) Characterising the digital twin: A systematic literature review, *CIRP Journal of Manufacturing Science and Technology*, 29, 36–52, <https://doi.org/10.1016/j.cirpj.2020.02.002>
- [32] Aryan, A., Bosche, F., & Tang, P. (2021) Planning for terrestrial laser scanning in construction: A review, *Automation in Construction*, 125, 103551, <https://doi.org/10.1016/j.autcon.2021.103551>
- [33] Zakaria, A. (2016) *Study of 3D modelling using terrestrial laser scanner based on cloud to cloud and target to target registration process (Case study: Brahu Temple, Mojokerto)*, *Jurnal Teknik ITS*, 4(1), 1–6.
- [34] Hinks, T., Carr, H., Truong-Hong, L., & Laefer, D. F. (2013) Point cloud data conversion into solid models via point-based voxelization, *Journal of Surveying Engineering*, 139(2), 72–83, [https://doi.org/10.1061/\(ASCE\)SU.1943-5428.0000097](https://doi.org/10.1061/(ASCE)SU.1943-5428.0000097)
- [35] Shim, C. S., Dang, N. S., Lon, S., & Jeon, C. H. (2019). Development of a bridge maintenance system for prestressed concrete bridges using 3D digital twin model. *Structure and Infrastructure Engineering*, 15(10), 1319–1332. <https://doi.org/10.1080/15732479.2019.1620789>

- [36] Dang, N. S., & Shim, C. S. (2018) BIM authoring for an image-based bridge maintenance system of existing cable-supported bridges, *IOP Conference Series: Earth and Environmental Science*, 143, 012032, <https://doi.org/10.1088/1755-1315/143/1/012032>
- [37] Tran, V. D., Sharma, P., & Nguyen, L. H. (2023) Digital twins for internal combustion engines: A brief review, *Journal of Emerging Science and Engineering*, 1(1), 29–35, <https://doi.org/10.61435/jese.2023.5>
- [38] Shahzad, M., Shafiq, M. T., Douglas, D., & Kassem, M. (2022) Digital twins in built environments: An investigation of the Characteristics, Applications, and Challenges, *Buildings*, 12(2), 120, <https://doi.org/10.3390/buildings12020120>
- [39] Bedarf, P., Dutto, A., Zanini, M., & Dillenburger, B. (2021) Foam 3D printing for construction: A review of applications, materials, and processes, *Automation in Construction*, 130, 103861, <https://doi.org/10.1016/j.autcon.2021.103861>
- [40] Willkens, D. S., Liu, J., & Alathamneh, S. (2024) A case study of integrating terrestrial laser scanning (TLS) and building information modeling (BIM) in heritage bridge documentation: The Edmund Pettus Bridge, *Buildings*, 14(7), 1940, <https://doi.org/10.3390/buildings14071940>